

CoupeL-Ledru Aude (Orcid ID: 0000-0003-2097-5924)  
Miller AJ (Orcid ID: 0000-0003-0572-7607)  
Liang Yun-Kuan (Orcid ID: 0000-0001-5869-5931)

## Countering elevated CO<sub>2</sub> induced Fe and Zn reduction in *Arabidopsis* seeds

Peng Sun<sup>1,2</sup>, Jean-Charles Isner<sup>2</sup> (orcid ID 0000-0003-4504-4392), Aude CoupeL-Ledru<sup>2,3</sup> (orcid ID 0000-0003-2097-5924), Qi Zhang<sup>1</sup>, Ashley J. Pridgeon<sup>2</sup> (orcid ID 0000-0002-5592-0109), Yaqian He<sup>1</sup>, Paloma K. Menguer<sup>4,5</sup> (orcid ID 0000-0003-2464-759X), Anthony J. Miller<sup>5</sup>, Dale Sanders<sup>5</sup> (orcid ID 0000-0002-1452-9808), Steve P. Mcgrath<sup>6</sup>, Fonthip Noothong<sup>2</sup>, Yun-Kuan Liang<sup>1</sup> (orcid ID 0000-0001-5869-5931) and Alistair M. Hetherington<sup>2</sup> (orcid ID 0000-0001-6060-9203)

<sup>1</sup>State Key Laboratory of Hybrid Rice, Department of Plant Sciences, College of Life Sciences, Wuhan University, Wuhan, 430072, China; <sup>2</sup>School of Biological Sciences, Life Sciences Building, 24 Tyndall Avenue, Bristol, BS8 1TQ, UK; <sup>3</sup>LEPSE, INRAE, University of Montpellier, Institut Agro, Montpellier, 75338 Cedex 07, France; <sup>4</sup>Centro de Biotecnologia, Universidade Federal do Rio Grande do Sul, Porto Alegre, 91501970, Brazil; <sup>5</sup>John Innes Centre, Norwich Research Park, Norwich, NR4 7UH, UK; <sup>6</sup>Rothamsted Research, West Common, Harpenden, Hertfordshire, AL5 2JQ, UK

### Authors for correspondence:

Yun-Kuan Liang <http://orcid.org/0000-0001-5869-5931>

Tel: +86 27 68752363

Email: [ykliang@whu.edu.cn](mailto:ykliang@whu.edu.cn)

Alistair M. Hetherington <http://orcid.org/0000-0001-6060-9203>

Tel: +44 117 3941188

Email: [Alistair.Hetherington@bristol.ac.uk](mailto:Alistair.Hetherington@bristol.ac.uk)

Received : 22 July 2021

Accepted : 17 May 2022

**Key words:** Stomatal function, CO<sub>2</sub> signalling pathway, Zn and Fe, *Arabidopsis thaliana*, Alpha carbonic anhydrases.

### Summary

This article has been accepted for publication and undergone full peer review but has not been through the copyediting, typesetting, pagination and proofreading process which may lead to differences between this version and the [Version of Record](#). Please cite this article as doi: [10.1111/nph.18290](https://doi.org/10.1111/nph.18290)

This article is protected by copyright. All rights reserved.

- Growth at increased concentrations of CO<sub>2</sub> induces a reduction in seed Zn and Fe. Using *Arabidopsis thaliana*, we investigated whether this could be mitigated by reducing the elevated CO<sub>2</sub>-induced decrease in transpiration.
- We used an infrared imaging-based screen to isolate mutants in *At1g08080* that encodes ALPHA CARBONIC ANHYDRASE 7 (ACA7). *aca7* mutant alleles display wild type (WT) responses to Abscisic acid (ABA) and light but are compromised in their response to elevated CO<sub>2</sub>.
- *ACA7* is expressed in guard cells. When *aca7* mutants are grown at 1000ppm CO<sub>2</sub> they exhibit higher transpiration and higher seed Fe and Zn content than WT grown under the same conditions.
- Our data show that by increasing transpiration it is possible to partially mitigate the reduction in seed Fe and Zn content when *Arabidopsis* is grown at elevated CO<sub>2</sub>.

## Introduction

Stomata are microscopic pores found on most land plant leaf surfaces. They regulate the uptake of CO<sub>2</sub> from the atmosphere and the loss of water vapour from the plant. This is achieved by controlling the aperture of the stomatal pores and the number of stomata that develop on the leaf surface. As both of these parameters are controlled by environmental signals this permits the plant to adapt its gas exchange to suit the prevailing conditions (Hetherington & Woodward, 2003; Lawson & Matthews, 2020). One key signal that affects stomatal movement and development is the concentration of atmospheric CO<sub>2</sub> (reviewed in Zhang *et al.*, 2018; Engineer *et al.*, 2014). The concentration of CO<sub>2</sub> in the atmosphere is continuing to rise and there has been considerable effort made to understand the impact of this increase on plant growth and productivity (Rice *et al.*, 2021; Danielle *et al.*, 2021). In the context of the work described here, one of the consequences of an increase in atmospheric CO<sub>2</sub> concentration is a decrease in the accumulation of mineral micronutrients in the aerial parts of the plant, including the seed (Myers *et al.*, 2014; Hepworth *et al.*, 2015). This

is believed, in part, to be a consequence of an elevated CO<sub>2</sub>-induced reduction in transpirational water loss (Houshmandfar *et al.*, 2018). This plays out as a reduction in the delivery of mineral micronutrients to the aerial parts of the plant (McDonald *et al.*, 2002; McGrath & Lobell, 2013; Hepworth *et al.*, 2015; Dong *et al.*, 2018; Ujii *et al.*, 2019). This could have negative effects on plant growth and where crops are concerned could impact negatively on human or animal health. This is particularly serious in the case of Fe and Zn where around 60% and 30% of the world population suffer from deficiency of these two minerals (Anusha *et al.*, 2021). Accordingly, decreased accumulation of these elements in fodder crops or cereals for human consumption could have serious health consequences and are likely to exacerbate what has been referred to as “hidden hunger”, prevalent particularly in the countries of sub-Saharan Africa (Gashu *et al.*, 2021).

Elevated concentrations of atmospheric CO<sub>2</sub> can bring about a reduction in transpirational water loss by inducing reductions in the aperture/number of stomata that develop on the leaf surface or through both processes. Work over many years has sought to understand the signal transduction pathways responsible for bringing about these changes. Although there is agreement that there is a role for ABA in elevated CO<sub>2</sub>-induced stomata closure (Merilo *et al.*, 2013, Chater *et al.*, 2105; Dittrich *et al.*, 2019; Movahedi *et al.*, 2021), there is debate about the requirement (Merilo *et al.* 2013, Chater *et al.*, 2105; Dittrich *et al.*, 2019; Movahedi *et al.*, 2021) or lack of requirement for members of the ABA receptor family (PYR/PYL/RCAR) (Zhang *et al.*, 2020). Elevated CO<sub>2</sub> is known to induce a reduction of stomatal aperture using a signal transduction pathway that includes an increase in the cytosolic Ca<sup>2+</sup> concentration (Webb *et al.*, 1996), Reactive oxygen species (ROS) (Chater *et al.*, 2015), β-carbonic anhydrases 1 and 4 (CA1 and CA4) (Hu *et al.*, 2010), the MATE-type transport channel RESISTANT TO HIGH CO<sub>2</sub> 1 (RHC1) (Tian *et al.*, 2015), the mitogen-activated protein kinases MPK4 and MPK12 (Hörak *et al.*, 2016; Töldsepp *et al.*, 2018), the protein kinase HIGH TEMPERATURE 1 (HT1), the BIG protein (He *et al.*, 2018), and the SnRK2 protein kinase OPEN STOMATA 1 (OST1) (Hashimoto *et al.*, 2006; Tian *et al.*, 2015). Upon activation OST1 can target the S-type anion channel (SLAC1), which ultimately leads to the closure of stomata (Vahisalu *et al.*, 2008; Xue *et al.*, 2011; Tian *et al.*, 2015). It is worth noting that MPK12/4 has been suggested to play a role as a central node of stomatal CO<sub>2</sub> signalling by mediating the activity of HT1 rather than RCH1 (Hörak *et al.*, 2016; Töldsepp *et al.*, 2018) and there are recent data suggesting that OST1 might

not be activated by elevated CO<sub>2</sub> although basal OST1 activity may still be involved in the response (Hsu *et al.*, 2018; Zhang *et al.*, 2020).

The observation that long-term elevated CO<sub>2</sub> reduces stomatal density was first reported by Woodward (1987). Subsequently, the control of stomatal development by elevated concentrations of CO<sub>2</sub> has been shown to involve the *HIGH CARBON DIOXIDE (HIC)* gene that encodes a putative 3-ketoacyl CoA synthase (Gray *et al.*, 2000),  $\beta$ - carbonic anhydrases CA1 and CA4, and the CO<sub>2</sub> RESPONSE SECRETED PROTEASE (CRSP) which is able to cleave the pro-peptide EPIDERMAL PATTERNING FACTOR 2 (EPF2), a negative stomatal development regulator (Engineer *et al.*, 2014). In addition, there is evidence for a requirement for ABA and members of the PYL/PYR/RCAR family of receptors in this response too (Chater *et al.*, 2015).

Given the relationship between transpiration and micronutrient accumulation in the aerial parts of the plant (McDonald *et al.*, 2002; Hepworth *et al.*, 2015), we reasoned that by interfering with elevated CO<sub>2</sub>-induced reductions in transpiration we should be able to help mitigate the negative effects of elevated CO<sub>2</sub> on seed micronutrient accumulation. Accordingly, we decided to identify genetic loci involved in transpiration responses to elevated CO<sub>2</sub>. For these loci to have value in the crop situation, they must neither interfere with the uptake of CO<sub>2</sub>, nor impact on the ability of the plant to reduce stomatal conductance during times of reduced soil water availability.

To identify novel loci involved in stomatal CO<sub>2</sub> responses we carried out a forward genetic screen in *Arabidopsis* using infrared thermal imaging. This approach has been used previously by us and others to identify genes involved in stomatal responses to ABA (Merlot *et al.*, 2002), reduced relative humidity (Xie *et al.*, 2006) and CO<sub>2</sub> signalling (Hashimoto *et al.*, 2006; He *et al.*, 2018). Here we report the isolation of alpha carbonic anhydrase mutants (*aca7-1* and its allelic line *aca7-2*).

Carbonic anhydrases catalyse the interconversion of CO<sub>2</sub> and water into protons and bicarbonate ions and the reaction is reversible. The *Arabidopsis* genome contains 19 CA genes and these are divided into three groups: (alpha)  $\alpha$ CA (8 genes), (beta)  $\beta$ CA (6 genes) and (gamma)  $\gamma$ CA (5 genes). Each group is evolutionary distinct and their protein structures very different to each other (HewettEmmett & Tashian 1996; Fabre *et al.*, 2007; DiMario *et al.*, 2017, 2018). Previous work in *Arabidopsis* has revealed that the  $\beta$ CA genes are involved in the control of stomatal conductance and development by CO<sub>2</sub>, with these processes being partially impaired in the  *$\beta$ ca1 $\beta$ ca4* double mutant (Hu

*et al.*, 2010, 2015; Hõrak *et al.*, 2021).  $\beta$ CAs have also been implicated in the control of stomatal responses to CO<sub>2</sub> in maize and rice (Kolbe *et al.*, 2018; Chen *et al.*, 2017). When exposed to elevated CO<sub>2</sub>, *aca7* mutants display reduced stomatal closure, increased conductance and transpiration, and increased accumulation of seed Fe and Zn compared with wild type. However, they retain wild-type stomatal responses to ABA, light and darkness. Together, with the work on beta CA1 and 4 (Hu *et al.*, 2010, 2021; Hõrak *et al.*, 2021) these results emphasise the importance of carbonic anhydrase enzyme activity in guard cell CO<sub>2</sub> signalling and also show that manipulation of the *ACA7* gene can help mitigate the effects of elevated CO<sub>2</sub> on seed accumulation of Fe and Zn in *Arabidopsis*.

## **Materials and Methods**

### **Plant material and growth conditions**

*Arabidopsis thaliana* accession Columbia-0 (Col-0, N1092) was obtained from Nottingham *Arabidopsis* Stock Centre (NASC) and used in this study. *aca7-1* (SALK\_009792) and *aca7-2* (SALK\_013186), both in the Col-0 background, were obtained from NASC as SALK transfer Deoxyribonucleic acid DNA (T-DNA) homozygous knockout lines and verified by genomic DNA Polymerase Chain Reaction (PCR) and reverse transcription polymerase chain reaction (RT-PCR) for T-DNA insertion and transcriptional abundance, respectively. All primers used for RT-PCR and genomic DNA PCR are listed in Supp. Table S1. Prior to sowing on soil, seeds were surface sterilized by washing with 70 % (v/v) ethanol and rinsed 6 times with deionised water and then sowed in 3:1 mix of peat-based multipurpose compost (Sinclair Horticultural, UK) and silver sand (MonroSouth, UK) and stratified at 4 °C in the darkness for 2 days. They were then transferred to a plant growth cabinet (MicroClima, Snijders Scientific, The Netherlands) and grown under 22°C/20°C, day/night cycles at 70% relative humidity (RH) with a 10-h-light/14-h-dark photoperiod and irradiated with fluorescent tubes at 100  $\mu\text{mol m}^{-2}\text{s}^{-1}$  at either 400±24 ppm (ambient) CO<sub>2</sub> or 1000±40 ppm (elevated).

### **Mutant screening using infrared thermography**

To identify mutants that displayed aberrant stomatal responses to elevated CO<sub>2</sub>, infrared

thermography was used as described by Wang *et al.* (2004). Mutant lines of the SALK homozygous T-DNA collection, N27941, were obtained from NASC (Nottingham, UK). 3,211 individual T-DNA insertion mutant lines were screened in total. For each individual mutant line, three plants were grown until they were 4 weeks old at  $400 \pm 24$  ppm CO<sub>2</sub> level in a walk-in growth chamber (Reftch, The Netherlands) at 22 °C, 70 % relative humidity, with a 10-h-light/14-h-dark photoperiod and irradiated with fluorescent tubes at  $100 \mu\text{mol m}^{-2}\text{s}^{-1}$ . Infrared thermal images were taken before and after the plants were exposed to  $1000 \pm 40$  ppm CO<sub>2</sub> for 1 hour using a SC1000 thermal imaging camera (FLIR Systems Inc., USA). Infrared images were captured and analysed using ThermalCAM software (FLIR Systems Inc., USA). Any mutant that exhibited altered leaf surface temperature compared to wild type (WT) was marked for further study. After 2 weeks, leaf surface temperature of each of the selected mutants was measured again in response to elevated CO<sub>2</sub> (1000 ppm) using infrared thermography. Once the phenotype was confirmed, a minimum of 6 plants from each mutant line and one additional independent allele of each mutant were subjected to detailed thermal analysis. Leaf rosette thermal images were captured from WT and each mutant allele every 10 seconds for 1 h before and after exposure to elevated CO<sub>2</sub>. Rosette pixel data from thermal images were plotted and analysed by one-way Analysis of Variance (ANOVA) with Tukey analysis.

### **Stomatal aperture measurement bioassay**

Stomatal responses to elevated CO<sub>2</sub> were measured as described in Chater *et al.* (2015). Using 6–7 weeks old plants, epidermal peels were removed from the abaxial side of the youngest fully expanded, mature leaves and floated (cuticle facing upwards) in petri dishes containing 10 mM 2-(N-morpholino) ethanesulfonic acid (MES)/KOH, potential of hydrogen (pH) 6.20 for 30 mins pre-incubation, epidermal peels were transferred to petri dishes with CO<sub>2</sub> free air, 10 mM MES/KOH, 50 mM KCl, pH 6.15 at 22°C and irradiated with white light at a photosynthetic photon flux density (PPFD) of  $150 \mu\text{mol m}^{-2}\text{s}^{-1}$  for 2 hours. They were then transferred to fresh petri dishes containing, 10 mM MES/KOH 50 mM KCl, pH 6.15 at 22 °C under a PPFD of  $150 \mu\text{mol m}^{-2}\text{s}^{-1}$  and aerated with either 400 ppm or 1000 ppm CO<sub>2</sub> for 2 hours. For each genotype, 30 stomatal pores were measured per treatment in 6 separate replicated experiments (total stomatal number=180).

Accepted Article

To study stomatal closure induced by darkness or ABA, abaxial epidermises were removed from the youngest fully expanded mature leaves of 6–7 weeks old *Arabidopsis* plants and floated on equilibrium buffer (10 mM MES/KOH, pH 6.20 for 30 mins) first. After peeling, the epidermal strips were then transferred to petri dishes containing stomatal incubation buffer (10 mM MES/KOH, 50 mM KCl, pH 6.15) and illuminated at a photon flux density of  $150 \mu\text{mol}^{-2}\text{s}^{-1}$  for 2 hours. After 2 hours, the isolated pieces of epidermis were transferred into petri dishes containing  $1 \mu\text{M}$  or  $10 \mu\text{M}$  ABA in incubation buffer or covered with black tape (dark treatment) for a further 2 hours under the same PPF. After these treatments stomatal apertures were measured using an inverted microscope (Leica DM-IRB, Leica Microsystems, Germany) connected to a Charge-coupled Device (CCD) camera (JVC-TKC1381, JVC Ltd., Japan). For each genotype, 30 stomatal pores were measured per treatment in three separate replicated experiments (total stomatal number=90). All measurements were conducted blindly and totally random between genotypes. Statistical analyses were conducted using one-way ANOVA with Tukey analysis, significant differences at  $P \leq 0.05$ .

### Stomatal conductance measurements

Steady state stomatal conductance ( $g_s$ ), transpiration rate (E) and  $\text{CO}_2$  assimilation rate (A) of intact *Arabidopsis* leaves were measured using Li-6400XT and Li-6800 analysis systems (Li-COR, Lincoln, USA), using the 6400-40 and 6800-01A head mounts for the 6400 and 6800, respectively. The system was set to a flow rate at  $200 \mu\text{mol s}^{-1}$ , a fast impeller speed level, 40–50 % relative humidity,  $24^\circ \text{C}$  chamber temperature and a top parabolic aluminized reflector light (PAR) of  $100 \mu\text{mol m}^{-2} \text{s}^{-1}$ , with a  $\text{CO}_2$  level of either 400 ppm or 1000 ppm. The data logging interval was set to 30 s. For measuring individual *aca7-1*, *aca7-2* or WT plants, the youngest fully expanded mature leaf from a 7–8-week old plant (still attached) was placed in the measuring chamber for a total duration of 45 mins measuring time. To further calculate average  $g_s$ , E and A for each measured leaf, we further used data recorded during a 15-minute window (from 25 to 40 mins after the start of measurements), corresponding to a stabilization plateau for all three variables. 12–29 individual plants for each genotype under two different  $\text{CO}_2$  concentrations were measured randomly from three different sowing batches. Statistical analysis was performed using one-way ANOVA with Tukey post-hoc tests, significant

differences at  $P \leq 0.05$ .

A-intercellular  $\text{CO}_2$  concentration  $C_i$  curves was measured using Li-6400XT system (Li-COR, Lincoln, USA). The system was set to a flow rate at  $200 \mu\text{mol s}^{-1}$ , a fast impeller speed level, 40–50 % relative humidity,  $24^\circ \text{C}$  chamber temperature and a top parabolic aluminized reflector light (PAR) of  $100 \mu\text{mol m}^{-2} \text{s}^{-1}$ , with a  $\text{CO}_2$  level at 400 ppm for 7 mins at the starting points. After  $A$  was logged,  $\text{CO}_2$  level was stepwise decreased to 50 ppm via 4 steps (300 ppm, 200 ppm and 100 ppm). Then, the  $\text{CO}_2$  level was restored to 400 ppm and followed by  $\text{CO}_2$  level stepwise increasing to 1400 ppm through 5 steps (600 ppm, 800 ppm, 1000 ppm and 1200 ppm). Each steps last 7 mins and data points were recorded at the end of each step. 3 individual plants of each genotype were measured and the statistical analysis was performed using paired nonparametric Friedman analysis with Dunn's test.

$g_s$  curves for WT, *aca7-1* and *aca7-2* plants grown under ambient  $\text{CO}_2$  was measured using GFS-3000 gas-exchange system (Walz, Germany). The system was set to a flow rate of  $200 \mu\text{mol s}^{-1}$ , an impeller speed level of 5, 70% relatively humidity,  $22^\circ \text{C}$  chamber temperature and a top parabolic aluminized reflector light (PAR) of  $100 \mu\text{mol m}^{-2} \text{s}^{-1}$ ,  $\text{CO}_2$  level at 400 ppm for 17 mins before increased to 1000 ppm level for another 27 mins.  $g_s$  data points were logged during the entire measurements with 4 independent plants of each genotype. The statistical analysis was performed with the 9 data points in the bracket using paired Student's *t* test analysis for WT and *aca7-1*, WT and *aca7-2*, respectively.

### **Expression pattern of *ACA7* in *Arabidopsis* leaf and guard cell protoplasts**

Ribonucleic acid (RNA) was extracted from plant leaves and guard cell protoplasts using a Machery-Nagel Nucleospin II plant RNA extraction kit with DNase I treatment (Thermo Fisher Scientific, USA) as described in Pandey *et al.* (2002) and Isner *et al.* (2018). First strand (Complementary DNA) cDNA of  $1 \mu\text{g}$  total RNA was synthesized using a Reverse Transcription Kit with Ribonuclease (RNase) Inhibitor (Applied Biosystems, USA) according to the manufacturer recommendations. To avoid amplification from trace genomic DNA contaminations, PCR primers were designed to span exon-exon junctions. cDNA corresponding to 20 ng of total RNA

and 300 nM of each primer were used in RT-PCR reactions using these conditions: 94 °C for 3 mins, 29 three-step cycles at 94 °C for 30 secs and 55 °C for 30 secs and 72 °C for 1 min followed by a final extension step at 72 °C for 5 mins by using 10X DreamTaq PCR Master Mix (Thermo Fisher, USA). PCR products were separated in 1.0 % (w/v) agarose gels and imaged under UV light (UWP GelDoc-It, USA). A real-time polymerase chain reaction (qPCR) was performed as described (Kostaki *et al.*, 2020) with Brilliant III SYBR Green QPCR (Agilent Technologies, USA) and synthesized cDNA from above. Data were collected using the MxPro software (Agilent Technologies, USA). Three technical repeats were performed for each sample, and three biological repeats refer to three independent experiment, using different tissue samples. Primer sequences for qPCR experiments are provided in Supp. Table 1.

#### **GUS staining of *ACA7<sub>pro</sub>::GUS***

A 1,500-bp fragment of genomic sequence immediately upstream of the start codon of *ACA7* was PCR amplified and subcloned into plasmid pBI121, which harbors a reporter gene *uidA* encoding  $\beta$ -glucuronidase (GUS), before transformation into WT *Arabidopsis* via the floral dipping method (Clough & Bent, 1998). The T<sub>2</sub> seeds of *ACA7<sub>pro</sub>::GUS* line were selected on ½ Murashige and Skoog medium (MS) plates with 50  $\mu$ g/ml kanamycin. The positive seedlings were transplanted into soil in order to set seeds. 15-day old *ACA7<sub>pro</sub>::GUS* seedlings were fixed by soaking in 90% acetone on ice for 20 mins followed by three rounds of washing in wash solution (0.1 M Phosphate Buffered Saline-PBS, pH 7.0, 10 mM Ethylenediaminetetraacetic acid-EDTA, 2 mM potassium ferrocyanide, 2 mM potassium ferricyanide). The plant tissue was then infiltrated for 10 mins using a vacuum with 500  $\mu$ l GUS staining solution (0.1 M PBS, pH 7.0, 10 mM EDTA, 2 mM potassium ferrocyanide, 2 mM potassium ferricyanide, 1 mM X-Gluc, Solarbio, China), followed by over-night incubation at 37°C. Decolouring was carried out by incubation in 100% ethanol for 1 hour, followed by incubation in 70% ethanol for 1 hour before imaging and analysis using a stereo microscope (Nikon SMZ25, Japan) with 6.3X magnification and also an inverted microscope (Olympus IX71, Japan) using 40X objective. All primers used for plasmid construction are listed in Supp. Table 1.

#### **Effect of CO<sub>2</sub> on yield and seed micronutrients**

WT, *aca7-1* and *aca7-2* plants were grown at 400±24 ppm and 1000±40 ppm CO<sub>2</sub> from seed to seed in individual pots. Growth conditions were same as described above. *Arabidopsis* stems were bagged after bolting and dry mature seeds were collected from the bag for analysis. The weight of seed of each plant was recorded on an individual plant basis. In total, seeds from 5–17 plants of each genotype were analysed under two different CO<sub>2</sub> levels. 1000 seeds from 3 individual plants of each genotype grown at 400 and 1000 ppm CO<sub>2</sub> were weighed. Seed samples were digested with a nitric acid (88%)/perchloric acid (12%) mix in a closed-vessel microwave system (Milestone, Sorisole, Italy) and then oven dried at 60 °C for 5 days. Metal concentrations (Cd, Co, Cr, Cu, Fe, Mn, Mo, Ni, Ti, Zn) were determined by inductively coupled plasma optical emission spectroscopy (ICP-OES; Vista-Pro Axial, Varyan Pty Ltd. Mulgrave, Australia) at the School of Biological Sciences, University of East Anglia (Menguier *et al.*, 2018). Seed samples analysis was performed in triplicate on plant samples from each line.

#### **Stomatal density and index assays**

Stomatal density and indices were recorded and calculated using fully expanded mature leaves when the plants started bolting (9–10 weeks old). Assays were performed using a single fully expanded leaf from 20 individual plants of each genotype grown under the 2 different CO<sub>2</sub> growth conditions from 3 separate batches of plants. Leaf impressions were made using dental resin (Light Body type 3, HUGE, China) which was applied to the abaxial surface, and then left at room temperature for 60 mins to dry. Transparent nail varnish was brushed on top of the resin impression and when set, transferred to a microscope slide using scotch tape (Scotch® crystal clear tape, 3M, USA) and imaged with a 20× objective (Olympus IX71, Japan) and CCD camera (JVC-TKC1381, JVC Ltd., Japan). Images of leaf impressions were taken from the centre area of the leaf blade and stomatal number and epidermal cell number were analysed using ImageJ (National Institute of Health, USA). 1 mm<sup>2</sup> stomatal density and stomatal indices were calculated as described in Chater *et al.* (2010). Statistics were performed using one-way ANOVAs with Tukey analysis, significant differences at P≤ 0.05.

#### **ACA7 protein carbonic anhydrase enzyme assay *in vitro***

ACA7 protein was expressed in *E. coli* and purified according to Isner *et al.* (2018).

Carbonic anhydrase activity was measured using the electrometric method as described by Wilbur & Anderson (1948). The assay was performed with 0–4 °C chilled 0.02 M 2-Amino-2-hydroxymethyl-propane-1,3-diol-HCl (Tris-HCl) (pH 8.3) buffer and CO<sub>2</sub>-saturated water. 4 ml CO<sub>2</sub>-saturated water was injected into 6 ml Tris-HCl buffer and the time taken for the pH to drop from 8.3 to 6.3 was recorded as T<sub>0</sub>. The carbonic anhydrase activity assay was performed using fresh buffer, fresh CO<sub>2</sub>-saturated water and 10 µl of 0.1 µg/µl glutathione S-transferase (GST) or GST:ACA7 protein, and the time taken for the pH to drop from 8.3 to 6.3 was recorded as T. One reading was taken for each protein sample and 5 protein samples of either GST protein or GST:ACA7 were assayed. The formula used to determine carbonic anhydrase activity was: units/µg of enzyme = 2 \* (T<sub>0</sub>-T) / (T \* µg protein in reaction mixture).

### Box plot figures and statistical analyses

In Box plot figures, the boxes are representing interquartile ranges and the whiskers are in Tukey style which are indicating data within 1.5 \* interquartile range. Unpaired Student's *t* test was used to test 2 samples and nonparametric test Kruskal-Wallis or ANOVA were used when with Dunn or Tukey post hoc analysis if more than 2 samples were involved. Shapiro-Wilk test was used to test the normality and the homoscedasticity of the different samples. The significance was denoted with letters in a  $p < 0.05$  manner unless stated otherwise.

## Results

### ***ACA7* is expressed in guard cells and *aca7* mutants display lower leaf surface temperatures than WT under elevated concentrations of CO<sub>2</sub>.**

To identify genes involved in stomatal CO<sub>2</sub> signaling pathways we carried out a forward genetic screen under 1000 ppm (elevated) atmospheric concentrations of CO<sub>2</sub> using a collection of 3,211 SALK homozygous T-DNA mutants (purchased from Nottingham *Arabidopsis* stock centre, NASC). Results of the screen are described in full in Supplemental Table 2 and the accompanying legend. Using this approach, we identified *aca7-1* on the basis of its reduced elevated CO<sub>2</sub>-induced leaf surface temperature increase (0.19–0.25°C lower than wild type) (Fig. 1a). The *aca7-1* mutant carries a T-DNA insertion in the 5<sup>th</sup> exon of *ATIG08080* that encodes the protein ALPHA

CARBONIC ANHYDRASE 7 (Supp. Fig. 1a). An allelic line of the *aca7-1* mutant known as *aca7-2*, with a T-DNA insertion in the 2<sup>nd</sup> exon of the gene was obtained from NASC as well (Supp. Fig. 1a). No full-length transcript of *ACA7* was detected in either *aca7-1* or *aca7-2* (Fig. 2a). *aca7-2* T-DNA insertion site is relatively close to the ATG start codon, which likely results in more efficient transcript disruption than *aca7-1*. *In vitro*, carbonic anhydrase activity assays demonstrate that the *ACA7* protein exhibits carbonic anhydrase activity (Fig. 1b). GUS staining of *ACA7*<sub>pro::GUS</sub> stable transgenic lines suggests that *ACA7* promoter activity is present in the vascular system and guard cells of 15-day old *Arabidopsis* plants (Fig. 1c). The expression of *ACA7* in guard cells and fully expanded mature leaves was confirmed by detecting *ACA7* expression in guard cell protoplasts and whole leaf RNA using RT-PCR and qPCR respectively (Supp. Fig. 1b; Supp. Table 3).

**Elevated CO<sub>2</sub>-induced reductions in stomatal aperture, conductance and transpiration are reduced in the *aca7* mutants compared with wild type. However, *aca7* mutants retain wild type responses to light, ABA and darkness.**

Using epidermal peel stomatal bioassays, we found that *aca7* mutants display wild type light-induced stomatal opening, dark-induced stomatal closure and ABA-induced stomatal closure responses (Fig. 2b, c). In contrast to WT, *aca7-1* shows reduced closure when exposed to 1000 ppm CO<sub>2</sub> while *aca7-2* fails to exhibit any closure (Fig. 2d). To facilitate comparison with previous work, we confirmed that neither *aca7-1* nor *aca7-2* show reduced stomatal apertures in response to 1000 ppm CO<sub>2</sub> by following the stomatal aperture measurement protocol used by Hu *et al.* (2010) (Supp. Fig. 1c). To investigate long-term effects of CO<sub>2</sub> on stomatal function, *aca7* mutants and wild type were grown in parallel at 1000 and 400 ppm CO<sub>2</sub> for 7–8 weeks. At 1000 ppm CO<sub>2</sub> *aca7* mutants displayed higher leaf transpiration (E) and stomatal conductance (g<sub>s</sub>) than wild type. In contrast, at 400 ppm CO<sub>2</sub> there were neither differences in transpiration nor conductance between the mutants and WT (Fig. 2e, f). Interestingly, the photosynthetic assimilation rates (A) of *aca7-1* and *aca7-2* remain similar to wild type regardless of the concentration of CO<sub>2</sub> (Fig. 2g), as a result, *aca7* mutants have lower intrinsic water use efficiency (WUE) relative to wild type at 1000±40 ppm CO<sub>2</sub>. In contrast, there is no difference in intrinsic WUE between wild type and mutants at 400

ppm CO<sub>2</sub> (Fig. 2h). To examine whether mutations in the *ACA7* gene impacted negatively on mesophyll conductance, we compared A-Ci curves between mutants and wild type. The data presented in Supplemental Fig. 2a, show that there are no differences between the mutants and wild type indicating that mesophyll conductance is not affected by mutations in the *ACA7* gene. We also used stepwise changed CO<sub>2</sub> level to investigate stomatal conductance of the mutants and wild type in a step change of CO<sub>2</sub> from 400 ppm to 1000 ppm CO<sub>2</sub>. The results are presented as Supp. Fig. 3b which reveal that the *aca7* mutants are less sensitive to CO<sub>2</sub>-induced stomatal closure than wild type.

### ***ACA7* is involved in the stomatal development response to elevated CO<sub>2</sub>.**

In response to growth at 1000 ppm CO<sub>2</sub>, both stomatal density and index were reduced in wild type (Fig 3a, b). In contrast, in the mutants there were no significant differences between stomatal indices when they were grown under 400 ppm or 1000 ppm CO<sub>2</sub> (Fig 3b). In the case of stomatal density, neither *aca7* mutant displays a 1000 ppm CO<sub>2</sub>-induced reduction and there is no significant difference between *aca7-2* and WT at 1000 ppm (Fig. 3a), strongly indicating that there is a role for *ACA7* in the stomatal development response to elevated CO<sub>2</sub>.

### **Elevated CO<sub>2</sub>-induced decreases in *Arabidopsis* seed Zn and Fe are reduced in *aca7* mutants compared with wild type.**

When we grew wild type under 1000 ppm CO<sub>2</sub> we observed a reduction in seed Fe, Zn (Fig. 4a,b), Mn, Ni, Cd, Cu and P compared with the contents recorded at 400 ppm CO<sub>2</sub> (Supp. Fig. 2c,e,f,g,j). There were no statistically significant differences recorded for Cr, Co, Mo or Ti (Supp. Fig. 2d,h,i,k). When we grew the *aca7* mutants at 400 and 1000 ppm CO<sub>2</sub>, although we saw a reduction in Fe and Zn at 1000 ppm, the reduction was much less than wild type. In WT, the Fe content at 1000 ppm CO<sub>2</sub> was 60.4% less than at 400 ppm, while in *aca7-1* and *aca7-2*, the reduction is only 35.9% and 23% respectively. In the case of Zn, the reduction in WT was 57.7%, while in *aca7-1* and *aca7-2* the decreases were 40.8% and 31%, respectively. The same trends in WT and *aca7-1* were observed for Mn, Ni, Cd Cu and P (Supp. Fig. 2c,e,f,g,j). However, in the

Accepted Article

case of the mutants, there were no statistically significant reduction between 400 ppm to 1000 ppm CO<sub>2</sub> (Supp. Fig. 2c,e,f,g,j). Together, these results show that disruption of the *ACA7* gene partially mitigates the effects of growth at 1000 ppm CO<sub>2</sub> on the accumulation of seed micronutrients. It is interesting to note that *aca7* mutants exhibit no increase in seed yield compared with WT when grown under 1000 ppm CO<sub>2</sub> (*aca7* mutants have lower seeds yield compared with WT under 1000 ppm CO<sub>2</sub> growth environment), reflecting the fact that less seed were produced (Supp. Fig. 2a,b).

### Discussion

Using an infrared thermal imaging-based forward genetic screen we found that the *ACA7* locus is involved in the regulation of stomatal development and function by 1000 ppm CO<sub>2</sub> (Fig. 2 and Fig. 3). We showed that *ACA7* encodes an alpha carbonic anhydrase ( $\alpha$ CA) enzyme, which catalyses the interconversion of CO<sub>2</sub> and bicarbonate (HCO<sub>3</sub><sup>-</sup>) and is expressed in guard cells (Fig. 1b, c).

Recent work on the *Arabidopsis beta1beta4* concluded that  $\beta$ -carbonic anhydrases have a significant role in mediating the stomatal closure response induced by transitions from 100–400 ppm CO<sub>2</sub>. In response to a transition of 400–800 ppm CO<sub>2</sub> the double mutant closed its stomata slower than wild type and overall, while significant the impact of lacking the  $\beta$ CAs was smaller at high CO<sub>2</sub> (Hörak *et al.*, 2021). It is interesting that we observed impaired responses to 1000 ppm CO<sub>2</sub> in *aca7*, whereas lesions in CO<sub>2</sub>-induced stomatal closure were only observed in *beta1beta4* (Hu *et al.*, 2010, 2015; Hörak *et al.*, 2021). One might imagine that  $\beta$ CAs could compensate for the loss of an *alpha CA*. The lack of compensation might reflect *ACA7* and *Beta1*, *Beta4* being expressed in different cellular compartments or that *ACA7* has other unknown functions or protein partners that cannot be complemented by *Beta1*, *Beta4*. In the context of the current investigation this is important because we are interested in mediating the effects of above ambient CO<sub>2</sub> on micronutrient acquisition and this response is partially compromised in the *aca7* mutants. In addition, for our results to have future relevance to a field situation it is important that stomata should continue to exhibit wild type responses to variables such as light and soil water status, which exert significant effects on crop performance and yield. As such, the fact that the *aca7* mutants display wild type aperture responses, at least in the short term, to ABA, light and darkness (Fig. 2b, c) suggests that these responses will be retained in the field situation. Accordingly, in

this investigation we add a member of the  $\alpha$ CA family to the list of CAs involved in the control of stomatal development.

Our primary aim was to investigate whether we could mitigate the elevated CO<sub>2</sub>-induced reduction in the accumulation of seed micronutrients by identifying mutants that maintain higher transpiration rates than wild type when grown at 1000 ppm CO<sub>2</sub>. The data in Fig. 2e and 2f show that the *aca7* mutants exhibited higher rates of transpiration and stomatal conductance than wild type, when grown at 1000 ppm CO<sub>2</sub> for 7–8 weeks. Importantly, photosynthetic assimilation (Fig. 2g) was maintained at wild type levels. In addition, because the drop in stomatal density was smaller in the *aca7* mutants than that observed in wild type at elevated CO<sub>2</sub> (Fig. 3a) this could also contribute to the increasing of transpiration. As would be expected these differences play out as a drop in water use efficiency in the mutants at elevated CO<sub>2</sub> as compared with wild type (Fig. 2h).

When we compared the *aca7* mutants with wild type grown from seed to seed in elevated CO<sub>2</sub>, although we saw a reduction in seed Fe and Zn compared with wild type grown at 400 ppm CO<sub>2</sub>, the decrease was not as great as wild type (Fig. 4a, b). These data suggest that manipulating the *ACA7* gene has the potential to, at least partially, mitigate the negative effects of growth at elevated CO<sub>2</sub> on seed micronutrient accumulation. There is, however, a penalty to pay, as our data reveal that *aca7* seed yield at elevated CO<sub>2</sub> was reduced compared with wild type when grown at 1000 ppm (Supp. Fig. 2a). When we investigated this in more depth and compared the weight of 1000-seed, we found that it was similar to wild type (Supp. Fig. 2b). This suggests that, rather than *aca7* seeds being smaller than wild type, the explanation for the lack of elevated CO<sub>2</sub>-induced increase in seed yield in *aca7* is more likely due to a reduction in the number of seed produced by the mutant when grown at elevated CO<sub>2</sub>.

Our stimulus in initiating the present study was a 2014 meta-analysis of the seed micronutrient levels of multiple crop species, which demonstrated that food crops including C<sub>3</sub> dicot (Field peas and Soybeans) and C<sub>3</sub> monocot (Wheat and Rice) had significantly reduced Fe and Zn levels in seeds when their growth conditions were changed from 385 ppm to 536 ppm CO<sub>2</sub> (Myers *et al.*, 2014). In this study, we have shown that through manipulating the expression of *ACA7* we can, in the case of Fe, Zn, Mn, Ni, Cd and Cu, partially mitigate the negative effect of elevated CO<sub>2</sub> on *Arabidopsis* seed micronutrient accumulation. We conclude that this has likely been

Accepted Article

achieved by reducing the extent of the elevated CO<sub>2</sub>-induced reduction in transpiration by interfering with the activity of the ACA7 enzyme. Having said this, and even though, based on our data we feel that the results we see here are due to an increase in transpiration driving increased Fe and Zn transport to the seed, it is possible that bundle sheath cells contribute to the accumulation of seed Fe and Zn. This is because, the data in Fig 1c show ACA7 promoter::GUS expression in vascular tissue. This is relevant because bundle sheath cells have been shown to regulate hydraulic conductance and ion distribution in the leaf (Shatil-Cohen & Moshelion, 2012). Although we cannot exclude the possibility that “carbohydrate dilution” is also involved in this phenotype, we feel that it is less likely because photosynthetic assimilation is unaffected in *aca7* (Fig. 3g) and dry matter accumulation at 1000 ppm was not significantly increased in *aca7-2* compared with wild type (Supp. Fig. 1d). It is also interesting that in our analysis that seed Cr, Co, Mo, P and Ti levels were unaffected by growth at 1000 ppm CO<sub>2</sub> in wild type indicating that while transpiration rates are important in the accumulation of some micronutrients this is not universally true (McGrath & Lobell, 2013).

In summary, we report the identification of the *ACA7* gene in *Arabidopsis* that plays a role in 1000 ppm CO<sub>2</sub>-mediated reduction in stomatal aperture. *ACA7* is widely expressed in guard and other cells. *aca7* mutants display defective 1000 ppm CO<sub>2</sub>-induced stomatal closure and transpiration responses but show wild type responses to ABA, light and darkness. When grown at 1000 ppm CO<sub>2</sub>, *aca7* mutants display reduced water use efficiency and seed yield compared with wild type. We set out to investigate whether we could mitigate the detrimental effects of 1000 ppm CO<sub>2</sub> on the accumulation of micronutrients including Fe and Zn by manipulating transpiration. In this we were successful, however, it will be interesting to investigate whether the strategy adopted here will be successful when applied to crop species.

### Acknowledgements

This work was supported by grants to A.M.H. from the UK Biotechnology and Biological Sciences Research Council (BBSRC), Grant No. BB/N001168/1 and the Leverhulme Trust. Y.-K. L. was supported by the National Natural Science Foundation of China under Grant No. 31770282. A.J.P. is grateful to the UK Biotechnology and Biological Sciences Research Council for a PhD studentship funded through the South West Biosciences Doctoral Training Partnership [training grant reference: BB/M009122/1]. A.C.-L. received an individual Marie Curie Fellowship (MSCA-IF

H2020). The CAPES Foundation within the Ministry of Education in Brazil programme 'Science without Borders' supported P.K.M., D.S. and A.J.M. were supported by grants BB/P004474/1, BB/J00PR9796 and BB/J000PR9799 from the Biotechnology and Biological Sciences Research Council (BBSRC) and the John Innes Foundation.

### Author contributions

A.M.H. and Y.-K.L. directed the study. P.S., Y.-K.L. and A.M.H. designed the research. P.S., J.-C.I., A.J.M., A.C.-L., Q.Z., Y.H., F.N. and P.K.M. conducted the experiments. P.S., J.-C.I., A.J.M., A.C.-L., Q.Z., A.J.P., S.P.M., D.S., P.K.M., Y.-K.L. and A.M.H. analyzed the data. A.M.H., P.S., Y.-K.L., A.J.P., A.C.-L. and A.J.M. wrote the manuscript. All authors read and approved the manuscript.

### Data availability

The data that support the findings of this study are available from the corresponding authors, Y.-K.L. and A.M.H., upon request.

### Supporting Information

**Supp. Fig. 1** *Arabidopsis ALPHA CARBONIC ANHYDRASE 7* gene can be amplified in guard cell cDNA using RT-PCR. *ALPHA CARBONIC ANHYDRASE 7* knock-out mutants (*aca7-1* and *aca7-2*) have reduced elevated CO<sub>2</sub>-induced stomatal closure and there is no difference in *aca7-2* dry weight grown under either 400 ppm or 1000 ppm CO<sub>2</sub>.

**Supp. Fig. 2** Micronutrient content of *Arabidopsis ALPHA CARBONIC ANHYDRASE 7* knock-out mutants (*aca7-1* and *aca7-2*) mutants and wild type (WT) grown under 400 ppm and 1000 ppm CO<sub>2</sub>.

**Supp. Figure 3.** Mean photosynthesis rate (A)- intercellular CO<sub>2</sub> concentration (Ci) curves for mesophyll conductance and stomatal conductance (g<sub>s</sub>) curves of CO<sub>2</sub> changes from 400 to 1000 ppm for *Arabidopsis ALPHA CARBONIC ANHYDRASE 7* knock-out mutants (*aca7-1* and *aca7-2*) mutants and wild type (WT).

**Supp. Table 1.** Primer sequences used in this study.

**Supp. Table 2.** The initial outcome of the thermal imaging screen.

**Supp. Table 3.** C<sub>t</sub> values of *Arabidopsis ALPHA CARBONIC ANHYDRASE 7* gene amplified by real-time polymerase chain reaction (qPCR) using *Arabidopsis* leaf cDNA as template.

## References

- Anusha G, Rao DS, Jaldhani V, Beulah P, Neeraja CN, Gireesh C, Anantha MS, Suneetha K, Santhosha R, Prasad ASH, Sundaram RM, Madhav MS, Fiyaz A, Brajendra P, Tuti MD, Bhavé MHV, Krishna KVR, Ali J, Subrahmanyam D, Senguttuvel P. 2021. Grain Fe and Zn content, heterosis, combining ability and its association with grain yield in irrigated and aerobic rice. *Scientific Reports* 11: 10579.
- Chater C, Peng K, Movahedi M, Dunn JA, Walker HJ, Liang YK, McLachlan DH, Casson S, Isner JC, Wilson I, Neill SJ, Hedrich R, Gray JE, Hetherington AM. 2015. Elevated CO<sub>2</sub>-induced responses in stomata require ABA and ABA signaling. *Current Biology* 25: 2709–2716.
- Chen T, Wu H, Wu J, Fan X, Li X, Lin Y. 2017. Absence of OsbetaCA1 causes a CO<sub>2</sub> deficit and affects leaf photosynthesis and the stomatal response to CO<sub>2</sub> in rice. *Plant Journal* 90: 344–357.
- Clough SJ, Bent AF. 1998. Floral dip: A simplified method for Agrobacterium-mediated transformation of *Arabidopsis thaliana*. *Plant Journal* 16: 735–743.
- DiMario RJ, Clayton H, Mukherjee A, Ludwig M, Moroney JV. 2017. Plant carbonic anhydrases: structures, locations, evolution, and physiological roles. *Molecular Plant* 10: 30–46.
- DiMario RJ, Machingura MC, Waldrop GL, Moroney JV. 2018. The many types of carbonic anhydrases in photosynthetic organisms. *Plant Science* 268: 11–17.
- Dittrich M, Mueller HM, Bauer H, Peirats-Llobet M, Rodriguez PL, Geilfus CM, Carpentier SC, Al Rasheid KAS, Kollist H, Merilo E, Herrmann J, Muller T, Ache P, Hetherington AM, Hedrich R. 2019. The role of *Arabidopsis* ABA receptors from the PYR/PYL/RCAR family in stomatal acclimation and closure signal integration. *Nature Plants* 5: 1002–1011.
- Dong J, Gruda N, Lam SK, Li X, Duan Z. 2018. Effects of elevated CO<sub>2</sub> on nutritional quality of vegetables: a review. *Frontiers in Plant Science* 9: 924.
- Engineer CB, Ghassemian M, Anderson JC, Peck SC, Hu H, Schroeder JI. 2014. Carbonic anhydrases, EPF2 and a novel protease mediate CO<sub>2</sub> control of stomatal development. *Nature* 513: 246–250.
- Fabre N, Reiter IM, Becuwe-Linka N, Genty B, Rumeau D. 2007. Characterization

and expression analysis of genes encoding alpha and beta carbonic anhydrases in *Arabidopsis*. *Plant, Cell & Environment* **30**: 617–629.

**Gashu D, Nalivata PC, Amede T, Ander EL, Bailey EH, Botoman L, Chagumaira C, Gameda S, Haefele SM, Hailu K, Joy EJM, Kalimbira AA, Kumssa DB, Lark RM, Ligowe IS, McGrath SP, Milne AE, Mossa AW, Munthali M, Towett EK, Walsh MG, Wilson L, Young SD, Broadley MR. 2021.** The nutritional quality of cereals varies geospatially in Ethiopia and Malawi. *Nature* **594**: 71–76.

**Gray JE, Holroyd GH, van der Lee FM, Bahrami AR, Sijmons PC, Woodward FI, Schuch W, Hetherington AM. 2000.** The HIC signalling pathway links CO<sub>2</sub> perception to stomatal development. *Nature* **408**: 713–716.

**Hashimoto M, Negi J, Young J, Israelsson M, Schroeder JI, Iba K. 2006.** *Arabidopsis* HT1 kinase controls stomatal movements in response to CO<sub>2</sub>. *Nature Cell Biology* **8**: 391–397.

**Hepworth C, Doheny-Adams T, Hunt L, Cameron D, Gray J. 2015.** Manipulating stomatal density enhances drought tolerance without deleterious effect on nutrient uptake. *New Phytologist* **208**: 336–341.

**He J, Zhang RX, Peng K, Tagliavia C, Li S, Xue S, Liu A, Hu H, Zhang J, Hubbard KE, Held K, McAinsh MR, Gray JE, Kudla J, Schroeder JI, Liang Y-K, Hetherington AM. 2018.** The BIG protein distinguishes the process of CO<sub>2</sub>-induced stomatal closure from the inhibition of stomatal opening by CO<sub>2</sub>. *New Phytologist* **218**: 232–241.

**Hetherington AM, Woodward FI. 2003.** The role of stomata in sensing and driving environmental change. *Nature* **424**: 901–908.

**HewettEmmett D, Tashian RE. 1996.** Functional diversity, conservation, and convergence in the evolution of the alpha-, beta-, and gamma-carbonic anhydrase gene families. *Molecular Phylogenetics & Evolution* **5**: 50–77.

**Hörak H, Sierla M, Töldsepp K, Wang C, Wang YS, Nuhkat M, Valk E, Pechter P, Merilo E, Salojärvi J, Overmyer K, Loog M, Brosché M, Schroeder JI, Kangasjärvi J, Kollist H. 2016.** A dominant mutation in the HT1 kinase uncovers roles of MAP kinases and GHR1 in CO<sub>2</sub>-Induced stomatal closure. *The Plant cell* **28(10)**: 2493–2509.

**Hörak H, Koolmeister K, Merilo E, Kollist H. 2021.** Concentration matters: different stomatal CO<sub>2</sub> responses at sub-ambient and above-ambient CO<sub>2</sub> levels. *bioRxiv*:

2021.2005.2013.443984.

- Houshmandfar, A, Fitzgerald, GJ, O’Leary, G, Tausz-Posch, S, Fletcher, A, Tausz, M. 2018.** The relationship between transpiration and nutrient uptake in wheat changes under elevated atmospheric CO<sub>2</sub>. *Physiologia Plantarum* **163**: 516–529.
- Hu H, Boisson-Dernier A, Israelsson-Nordstrom M, Bohmer M, Xue S, Ries A, Godoski J, Kuhn JM, Schroeder JI. 2010.** Carbonic anhydrases are upstream regulators of CO<sub>2</sub>-controlled stomatal movements in guard cells. *Nature Cell Biology* **12**: 87–93
- Hu HH, Rappel WJ, Occhipinti R, Ries A, Bohmer M, You L, Xiao CL, Engineer CB, Boron WF, Schroeder JI. 2015.** Distinct cellular locations of carbonic anhydrases mediate carbon dioxide control of stomatal movements. *Plant Physiology* **169**: 1168–1178.
- Hu Z, Ma Q, Foyer CH, Lei C, Choi HW, Zheng C, Li J, Zuo J, Mao Z, Mei Y, Yu J, Klessig DF, Shi K. 2021.** High CO<sub>2</sub>- and pathogen-driven expression of the carbonic anhydrase betaCA3 confers basal immunity in tomato. *New Phytologist* **229**: 2827–2843.
- Hsu PK, Takahashi Y, Munemasa S, Merilo E, Laanemets K, Waadt R, Pater D, Kollist H, Schroeder JI. 2018.** Abscisic acid-independent stomatal CO<sub>2</sub> signal transduction pathway and convergence of CO<sub>2</sub> and ABA signaling downstream of OST1 kinase. *Proceedings of the National Academy of Sciences of the United States of America* **115**: E9971–E9980.
- Isner JC, Olteanu VA, Hetherington AJ, Coupel-Ledru A, Sun P, Pridgeon AJ, Jones GS, Oates M, Williams TA, Maathuis FJM, Kift R, Webb AR, Gough J, Franklin KA, Hetherington AM. 2019.** Short- and long-term effects of UVA on *Arabidopsis* are mediated by a novel cGMP phosphodiesterase. *Current Biology* **29**: 2580–2585.
- Kolbe AR, Studer AJ, Cornejo OE, Cousins AB. 2019.** Insights from transcriptome profiling on the non-photosynthetic and stomatal signaling response of maize carbonic anhydrase mutants to low CO<sub>2</sub>. *BMC Genomics* **20**: 138.
- Kostaki KI, Coupel-Ledru A, Bonnell VC, Gustavsson M, Sun P, McLaughlin FJ, Fraser DP, McLachlan DH, Hetherington AM, Dodd AN, Franklin KA. 2020.** Guard cells integrate light and temperature signals to control stomatal aperture. *Plant Physiology* **182(3)**: 1404–1419.
- Lawson T, Matthews J. 2020.** Guard cell metabolism and stomatal function. *Annual*

*Review of Plant Biology* **71**: 273–302.

- McDonald EP, Erickson JE, Kruger EL. 2002.** Research note: Can decreased transpiration limit plant nitrogen acquisition in elevated CO<sub>2</sub>? *Functional Plant Biology* **29**: 1115–1120.
- McGrath M, Lobell B. 2013.** Reduction of transpiration and altered nutrient allocation contribute to nutrient decline of crops grown in elevated CO<sub>2</sub> concentrations. *Plant, Cell & Environment* **36**: 697–705.
- Menguer PK, Vincent T, Miller AJ, Brown JKM, Vincze E, Borg S, Holm PB, Sanders D, Podar D. 2018.** Improving zinc accumulation in barley endosperm using HvMTP1, a transition metal transporter. *Plant Biotechnology Journal* **16**: 63–71.
- Merilo E, Laanemets K, Hu H, Xue S, Jakobson L, Tulva I, Gonzalez-Guzman M, Rodriguez PL, Schroeder JI, Broschè M, Kollist H. 2013** PYR/RCAR receptors contribute to ozone-, reduced air humidity-, darkness-, and CO<sub>2</sub>-induced stomatal regulation. *Plant Physiology* **162**:1652–1668.
- Merlot S, Mustilli AC, Genty B, North H, Lefebvre V, Sotta B, Vavasseur A, Giraudat J. 2002.** Use of infrared thermal imaging to isolate *Arabidopsis* mutants defective in stomatal regulation. *Plant Journal* **30**: 601–609.
- Movahedi M, Zoulias N, Casson SA, Sun P, Liang Y-K, Hetherington AM, Gray JE, Chater CCC. 2021.** Stomatal responses to carbon dioxide and light require abscisic acid catabolism in *Arabidopsis*. *Interface Focus* **11**: 20200036.
- Myers SS, Zanobetti A, Kloog I, Huybers P, Leakey AD, Bloom AJ, Carlisle E, Dietterich LH, Fitzgerald G, Hasegawa T, Holbrook NM, Nelson RL, Ottman MJ, Raboy V, Sakai H, Sartor KA, Schwartz J, Seneweera S, Tausz M, Usui Y. 2014.** Increasing CO<sub>2</sub> threatens human nutrition. *Nature* **510**: 139–142.
- Pandey S, Wang X-Q, Coursol SA, Assmann SM. 2002.** Preparation and applications of *Arabidopsis thaliana* guard cell protoplasts. *New Phytologist* **153**: 517–526.
- Rice C, Wolf J, Fleisher DH, Acosta SM, Adkins SW, Bajwa AA, Ziska LH. 2021.** Recent CO<sub>2</sub> levels promote increased production of the toxin parthenin in an invasive *Parthenium hysterophorus* biotype. *Nature Plants* **7**: 725–729.
- Shatil-Cohen A, Moshelion M. 2012.** Smart pipes: the bundle sheath role as xylem-mesophyll barrier. *Plant Signaling & Behavior* **7**: 1088–1091
- Tian W, Hou C, Ren Z, Pan Y, Jia J, Zhang H, Bai F, Zhang P, Zhu H, He Y, Luo**

- S, Li L, Luan S. 2015. A molecular pathway for CO<sub>2</sub> response in *Arabidopsis* guard cells. *Nature Communication* 6: 6057.
- Töldsepp K, Zhang J, Takahashi Y, Sindarovska Y, Hőrak H, Ceciliato P, Koolmeister K, Wang YS, Vaahtera L, Jakobson L, Yeh CY, Park J, Brosche M, Kollist H, Schroeder JI. 2018. Mitogen-activated protein kinases MPK4 and MPK12 are key components mediating CO<sub>2</sub>-induced stomatal movements. *Plant Journal* 96: 1018–1035.
- Ujūe K, Ishimaru K, Hirotsu N, Nagasaka S, Miyakoshi Y, Ota M, Tokida T, Sakai H, Usui Y, Ono K, Kobayashi K, Nakano H, Yoshinaga S, Kashiwagi T, Magoshi J. 2019. How elevated CO<sub>2</sub> affects our nutrition in rice, and how we can deal with it. *PLoS One* 14: e0212840.
- Vahisalu T, Kollist H, Wang YF, Nishimura N, Chan WY, Valerio G, Lamminmaki A, Brosche M, Moldau H, Desikan R, Schroeder JI, Kangasjarvi J. 2008. SLAC1 is required for plant guard cell S-type anion channel function in stomatal signalling. *Nature* 452: 487–491.
- Wang Y, Holroyd G, Hetherington AM, Ng CK. 2004. Seeing 'cool' and 'hot'--infrared thermography as a tool for non-invasive, high-throughput screening of *Arabidopsis* guard cell signalling mutants. *Journal of Experimental Botany* 55: 1187–1193.
- Woodward FI. 1987. Stomatal numbers are sensitive to increases in CO<sub>2</sub> from preindustrial levels. *Nature* 327: 617–618.
- Xie XD, Wang YB, Williamson L, Holroyd GH, Tagliavia C, Murchie E, Theobald J, Knight MR, Davies WJ, Leyser HMO, Hetherington AM. 2006. The identification of genes involved in the stomatal response to reduced atmospheric relative humidity. *Current Biology* 16: 882–887.
- Xue SW, Hu HH, Ries A, Merilo E, Kollist H, Schroeder JI. 2011. Central functions of bicarbonate in S-type anion channel activation and OST1 protein kinase in CO<sub>2</sub> signal transduction in guard cell. *EMBO Journal* 30: 1645–1658.
- Zhang J, De-Oliveira-Ceciliato P, Takahashi Y, Schulze S, Dubeaux G, Hauser F, Azoulay-Shemer T, Toldsepp K, Kollist H, Rappel WJ, Schroeder JI. 2018. Insights into the molecular mechanisms of CO<sub>2</sub>-mediated regulation of stomatal movements. *Current Biology* 28: R1356–R1363.
- Zhang L, Takahashi Y, Hsu PK, Kollist H, Merilo E, Krysan PJ, Schroeder JI. 2020. FRET kinase sensor development reveals SnRK2/OST1 activation by

ABA but not by MeJA and high CO<sub>2</sub> during stomatal closure. *eLife* 9: e56351.

## Figure Legends

**Fig. 1 *Arabidopsis* ALPHA CARBONIC ANHYDRASE 7 is expressed in guard cells and exhibits carbonic anhydrase activity.** (a) Boxplots represent rosette surface temperature of *Arabidopsis* wild type (WT), ALPHA CARBONIC ANHYDRASE 7 gene knock-out mutants (*aca7-1* and *aca7-2*) when exposed to 400 ppm and 1000 ppm CO<sub>2</sub>; dots in the middle of the boxes represent the mean surface temperature, the upper and lower whiskers are plotted following Tukey method, the horizontal line in the middle of the box are representing median value. Significance was tested by one-way Analysis of Variance (ANOVA), P≤0.05, n=4; multiple comparison Tukey. The lowercase letters above boxplots are representing statistically significant relationships. (b) Boxplots represent carbonic anhydrase (CA) activity *in vitro*; dots in the middle of the boxes represent the mean CA activity, the upper and lower whiskers are plotted following Tukey method, the horizontal line in the middle of the box are representing median value. Significance was tested by Student's *t* test, \*\*\*, P≤0.0001, n=5. (c) β-glucuronidase (GUS) staining of 15 days old *ACA7*<sub>pro</sub>::GUS transgenic line showed that *ACA7* is expressed in cotyledons, the vascular system, and in guard cells.

**Fig. 2 *Arabidopsis* ALPHA CARBONIC ANHYDRASE 7 knock-out mutants (*aca7-1* and *aca7-2*) are impaired in elevated CO<sub>2</sub>-induced stomatal closure but not in their responses to darkness or Abscisic acid (ABA).** (a) In *Arabidopsis*, Reverse transcription polymerase chain reaction (RT-PCR) analysis shows that ALPHA CARBONIC ANHYDRASE 7 gene (*ACA7*) transcription is disrupted in gene knock-out mutants (*aca7-1* and *aca7-2*). Boxplots in (b) and (c) represent stomatal aperture of wild type (WT), *aca7-1* and *aca7-2* treated with darkness or ABA respectively; dots in the middle of the boxes represent the mean stomatal aperture, the upper and lower whiskers are plotted following Tukey method, the horizontal line in the middle of the box are representing median value. Significance was tested by one-way Analysis of Variance (ANOVA), P≤0.05, n=90; multiple comparison Tukey. The lowercase letters above boxplots are representing statistically significant relationships. (d) Boxplots represent stomatal apertures of WT, *aca7-1* and *aca7-2* under 0 ppm, 400 ppm and 1000 ppm CO<sub>2</sub>; dots in the middle of the boxes indicate mean stomatal apertures, the upper

and lower whiskers are plotted following Tukey method, the horizontal line in the middle of the box are representing median value. Significance was tested by one-way ANOVA,  $P \leq 0.05$ ,  $n=180$ ; multiple comparison Tukey. The lowercase letters above boxplots are representing statistically significant relationships. (e–h) Boxplots represent stomatal conductance ( $g_s$ ), transpiration (E), water use efficiency (WUE) and  $CO_2$  assimilation rate ( $A$ ) of WT, *aca7-1* and *aca7-2* grown for 7–8-weeks under 400 ppm or 1000 ppm  $CO_2$  respectively; dots in the middle of the boxes are represent mean values. Significance was tested by one-way ANOVA,  $P \leq 0.05$ ,  $n=12–29$ ; multiple comparison Tukey. The lowercase letters above boxplots are representing statistically significant relationships.

**Fig. 3 Effect of growth at 400 ppm and 1000 ppm  $CO_2$  on stomatal density and index on *Arabidopsis* ALPHA CARBONIC ANHYDRASE 7 knock-out mutants (*aca7-1* and *aca7-2*) mutants and wild type (WT).**

(a) Boxplots represent stomatal density of *Arabidopsis* WT, *aca7-1* and *aca7-2* grown for 9–10 weeks under 400 ppm or 1000 ppm  $CO_2$ ; dots in the middle of the boxes are represent mean values, the upper and lower whiskers are plotted following Tukey method, the horizontal line in the middle of the box are representing median value. Significance was tested by one-way Analysis of Variance (ANOVA),  $P \leq 0.05$ ,  $n=20$ ; multiple comparison Tukey. The lowercase letters above boxplots are representing statistically significant relationships. (b) Boxplots represent stomatal index of WT, *aca7-1* and *aca7-2* grown under 400 ppm  $CO_2$  or 1000 ppm  $CO_2$ ; dots in the middle of the boxes represent mean values, the upper and lower whiskers are plotted following Tukey method, the horizontal line in the middle of the box are representing median value. Significance was tested by one-way ANOVA,  $P \leq 0.05$ ,  $n=20$ ; multiple comparison Tukey. The lowercase letters above boxplots are representing statistically significant relationships.

**Fig. 4 Seed Fe and Zn content of *Arabidopsis* ALPHA CARBONIC ANHYDRASE 7 knock-out mutants (*aca7-1* and *aca7-2*) mutants and wild type (WT) mutants grown under 400 ppm and 1000 ppm  $CO_2$ .** Boxplots represent the (a) Fe or (b) Zn content levels in seeds of all genotypes under 400 ppm or 1000 ppm  $CO_2$  level; dots in the middle of the boxes represent mean content levels, the upper and lower whiskers

are plotted following Tukey method, the horizontal line in the middle of the box are representing median value. Significance was tested by Kruskal-Wallis nonparametric test,  $P \leq 0.05$ , Fe  $n=5-17$ , Zn  $n=5-18$ . The lowercase letters above boxplots are representing statistically significant relationships.

# Fig. 1

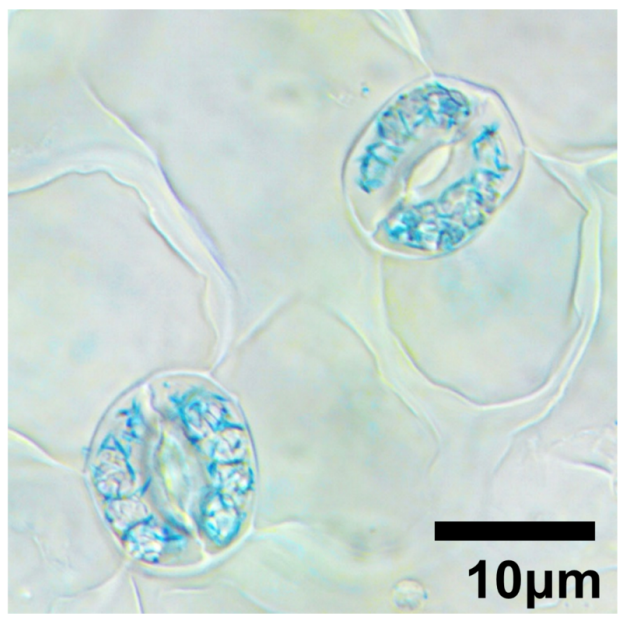
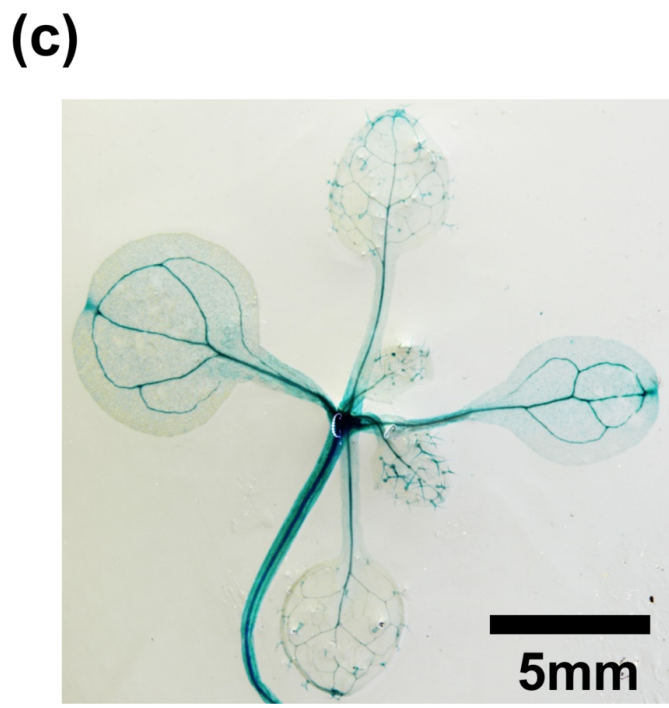
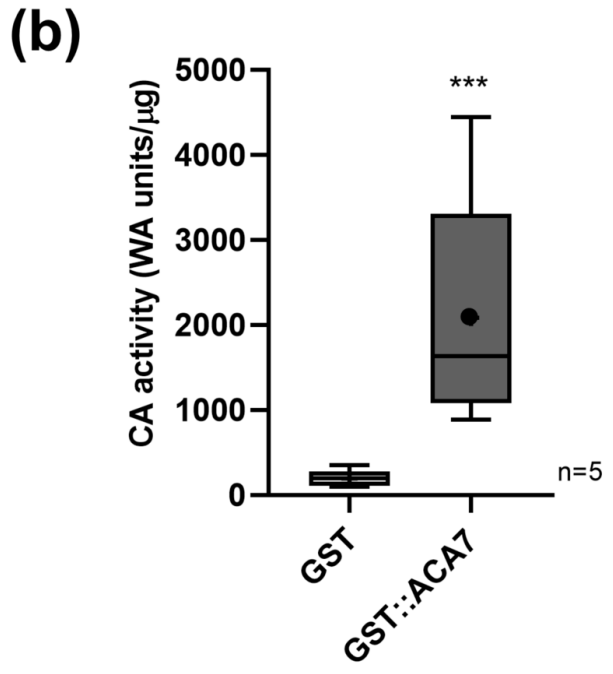
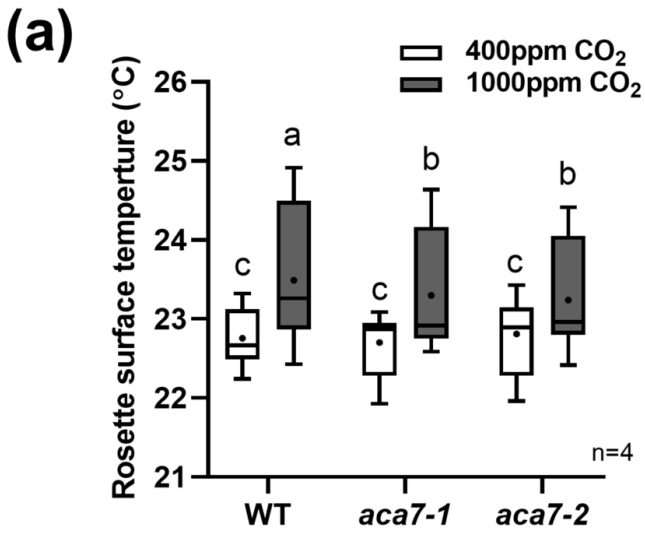


Fig. 2

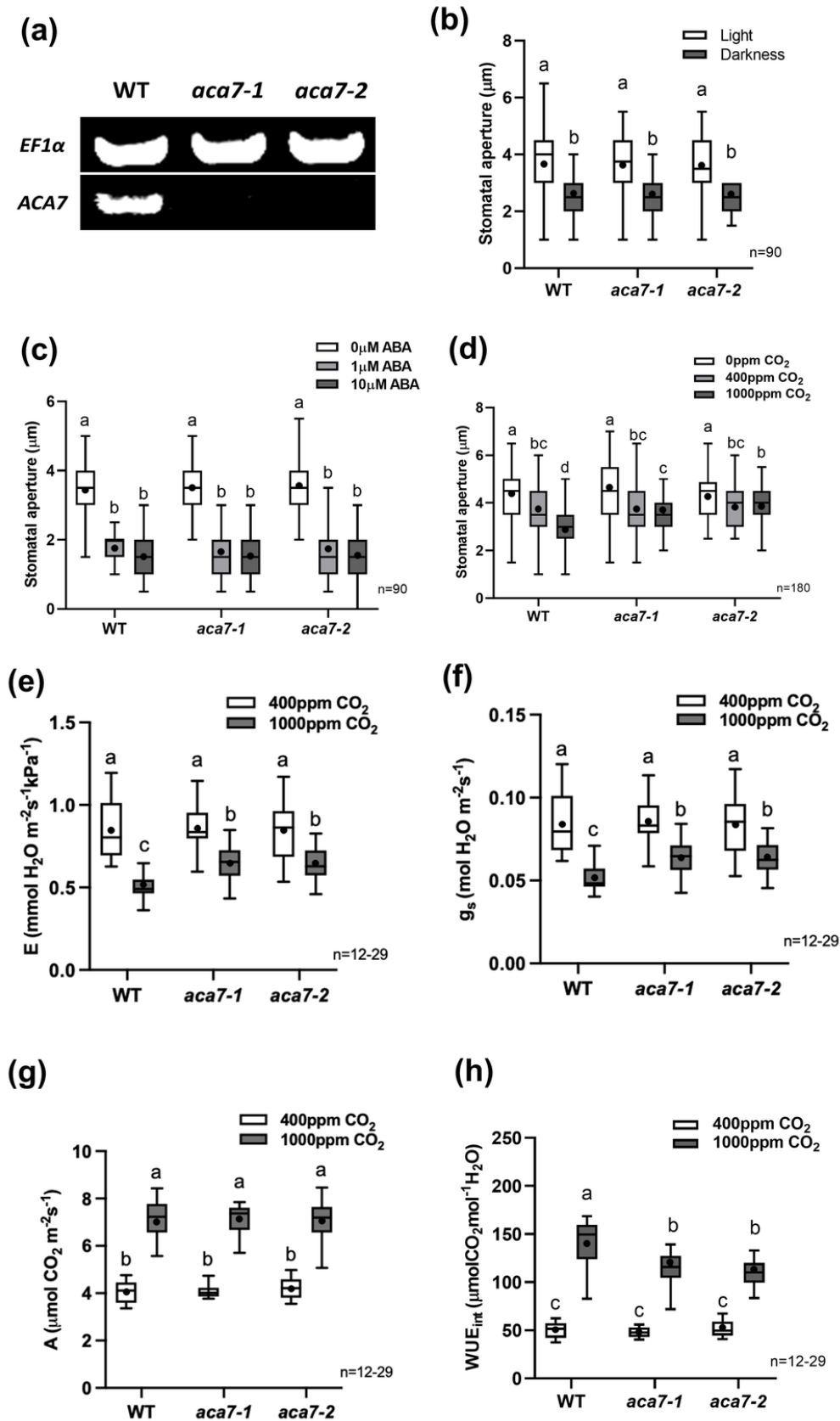
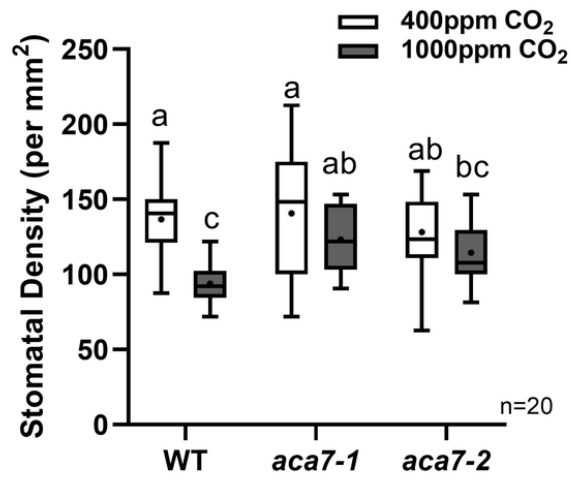


Fig. 3

(a)



(b)

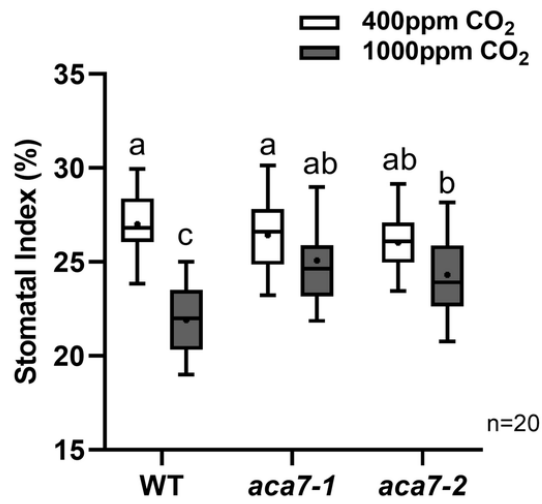


Fig. 4

